Astron. Nachr. / AN **337**, No. 1/2, 188 – 193 (2016) / **DOI** 10.1002/asna.201512289

AGN feedback and star formation in young and old radio galaxies*

A. Labiano[1,**], **S. García-Burillo**[2], **F. Combes**[3], **A. Usero**[2], **R. Soria-Ruiz**[2], **J. Piqueras López**[4], **G. Tremblay**[5,6], **L. Hunt**[7], **A. Fuente**[2], **R. Neri**[8], and **T. Oosterloo**[9,10]

[1] Institute for Astronomy, Department of Physics, ETH Zurich, CH-8093 Zurich, Switzerland
[2] Observatorio Astronómico Nacional, Alfonso XII, 3, 28014, Madrid, Spain.
[3] Observatoire de Paris, LERMA & CNRS: UMR8112, 61 Av. de l'Observatoire, 75014 Paris, France.
[4] Centro de Astrobiología (CSIC-INTA), Carretera de Ajalvir km. 4, 28850 Torrejón de Ardoz, Madrid, Spain.
[5] Department of Physics and Yale Center for Astronomy & Astrophysics, Yale University, 217 Prospect Street, New Haven, CT 06511, USA
[6] European Southern Observatory, Karl-Schwarzschild-Str. 2, 85748 Garching bei Munchen, Germany.
[7] INAF/Osservatorio Astrofisico di Arcetri, Largo Enrico Fermi 5, 50125 Florence, Italy.
[8] IRAM, 300 rue de la Piscine, Domaine Universitaire, 38406 St. Martin d'Héres Cedex, France.
[9] The Netherlands Institute for Radio Astronomy - ASTRON, Postbus 2, 7990 AA, Dwingeloo, The Nether;ands
[10] Kapteyn Astronomical Institute, University of Groningen, Postbus 800, 9700 AV Groningen, The Netherlands.

Received 2015 Oct 19, accepted 2015 Oct 21
Published online 2016 Feb 03

Key words galaxies: active – galaxies: individual: (3C 236, 3C 293) – Galaxies: ISM – galaxies: kinematics and dynamics – galaxies: star formation – ISM: jets and outflows

Powerful radio galaxies show evidence of ongoing active galactic nuclei (AGN) feedback, mainly in the form of fast, massive outflows. Yet, it is not clear how these outflows affect the star formation of their hosts. We investigated the different manifestations of AGN feedback in the evolved 3C 293 radio source, and in the young, reactivated 3C 236. Both sources harbor young star-forming regions and fast outflows of H I and ionized gas. Due to the different evolution stages of these sources, they are expected to be at different phases of the AGNISM interaction process. Using high spatial resolution observations of CO lines taken with the IRAM Plateau de Bure interferometer, we studied the distribution and kinematics of the molecular gas in these sources, and compared the results with the dust and star-formation images of the host. We searched for signatures of outflow motions in the CO kinematics, and derived the star formation rate (SFR) and star formation efficiency (SFE) of the host with all available SFR tracers. Based on the gas mass derived from our observations and on the SFR estimates, we compared the star-formation efficiency of 3C 236 and 3C 293 against a sample of powerful radio galaxies. Our results suggest that the apparently low SFE of evolved radio galaxies is not necessarily due to AGN feedback, but may be caused by an underestimation of the SFR and/or an overestimation of the molecular gas densities in radio galaxies.

1 Introduction

Powerful radio galaxies experience different manifestations of active galactic nuclei (AGN) feedback. The H I and ionized gas dynamics in their host galaxies at all redshifts show the presence of massive outflows, usually linked to the jets or the central source (e.g., Morganti et al. 2003a; Rupke et al. 2005; Holt et al. 2006; Nesvadba et al. 2006, 2008; Lehnert et al. 2011). Even though molecular gas could dominate the mass/energy budget of the wind, only one (4C 12.50; Dasyra & Combes 2011) radio galaxy shows evidence of a molecular outflow in its interstellar medium (ISM). Powerful radio galaxies also seem to have a diminished star formation efficiency (SFE), another manifestation of AGN feedback. The SFE of a galaxy can be defined as its star formation rate (SFR) per unit of molecular gas. Based on this definition, and the 7.7 μm polycyclic aromatic hydrocarbons (PAH) emission, Nesvadba et al. (2010) found that powerful radio galaxies form stars with efficiencies 10 to 50 times lower than galaxies that follow the canonical Kennicutt-Schmidt law (KS, Schmidt 1959; Kennicutt 1998b). It is thought that the presence of high-speed jet-induced shocks could increase the turbulence of the molecular gas which, in turn, would inhibit the star formation in the galaxy.

In these proceedings we present the current status of our research on the impact of AGN feedback in the ISM of powerful radio galaxies. We carried out interferometric observations with the Plateau de Bure Interferometer (PdBI, Guilloteau et al. 1992) and an extensive multi-wavelength archival search to investigate the impact of the AGN on its host. Using the 1 mm and 3 mm continuum, and the

* Based on observations carried out with the IRAM Plateau de Bure Interferometer. IRAM is supported by INSU/CNRS (France), MPG (Germany) and IGN (Spain).

** Corresponding author: alvaro.labiano@phys.ethz.ch

^{12}CO(1-0), ^{12}CO(2-1) lines, we studied the morphology and kinematics of the molecular gas in the radio galaxies 3C 236 and 3C 293. We searched for outflow signatures in the CO map, and compare the the results obtained with the evidence of outflow signatures in different ISM tracers. We measured the SFE of our sample, and make a comparison with the SFE of radio galaxies and normal star-forming galaxies to examine the possible impact of AGN feedback on star formation.

1.1 3C 236

3C 236 is the second largest radio galaxy in the Universe ($\sim$4.5 Mpc deprojected size, Barthel et al. 1985; Machalski et al. 2008; Willis et al. 1974). The radio maps of 3C 236 show a double-double morphology, consistent with a reignition of the AGN activity, probably due to a minor merger (O'Dea et al. 2001). The larger source is a 2.6×10^8 yr old Fanaroff-Riley type II (FR II, Fanaroff-Riley 1974) while the smaller source, which is 2 kpc in size, is a Compact Steep Spectrum (CSS) source with an age of a 0.1 Myr. Both are oriented at an angle $\sim30°$ to the plane of the sky, with the North-West jet approaching (Schilizzi et al. 2001). The host of 3C 236 is a massive elliptical galaxy which has probably undergone a minor merger. Optical-UV photometry shows several regions of recent star formation. Both the recent episode of radio activity and the star formation seem to have been triggered by the merger (O'Dea et al. 2001; Tadhunter et al. 2011; Tremblay et al. 2010). However, it is not completely clear how the nuclear stellar population relates to the AGN activity. Optical and radio spectra show that 3C 236 harbors a fast, massive outflow, seen as a blue-shifted absorption in the H I spectrum, and red- and blue-shifted wings in the ionized gas emission lines (Labiano et al. 2013; Morganti et al. 2005).

1.2 3C 293

3C 293 is a FR II (although it also shows FR I properties) radio galaxy with a size of $\sim$200 kpc and PA = 135°. The inner 2″ of the radio source show a compact core and two jets aligned east-west (PA = 93°), where the eastern jet is approaching (Floyd et al. 2006; Leipski et al. 2009; Massaro et al. 2010). Spectral aging estimations calculate the age of the large radio source to be $\leq$20 Myr, while the compact source is $\leq$0.18 Myr ago (Akujor et al. 1996; Joshi et al. 2011). The large radio source stopped its activity $\sim$0.35 Myr ago, while the time-lapse between the two activity epochs lasted only $\leq$0.1 Myr (Joshi et al. 2011). The short time lapse between radio activity episodes suggests that the radio jets of 3C 293 have probably interacted with the ISM during the whole life of the radio galaxy. The host galaxy of 3C 293 has been classified both as a spiral galaxy and as an elliptical galaxy. The optical and infrared images of 3C 293 show a dust disk, compact knots, and large dust lanes (de Koff et al. 2000; Papadopoulos et al. 2010), consistent with a gas-rich merger of an elliptical galaxy with a spiral galaxy (Capetti et al. 2000; de Koff et al. 2000; Martel et al. 1999). This merger probably triggered the recent star formation seen in near-UV (NUV) images of the host (Allen et al. 2008; Baldi & Capetti 2008; Tadhunter et al. 2011, 2005). The H I and optical spectra of 3C 293 show the presence of a fast outflow associated with the jets of the compact radio source (Emonts et al. 2005; Mahony et al. 2013; Morganti et al. 2005). Previous observations of the molecular gas in 3C 293 lacked the required velocity coverage and sensitivity to detect the outflow seen in H I and ionized gas.

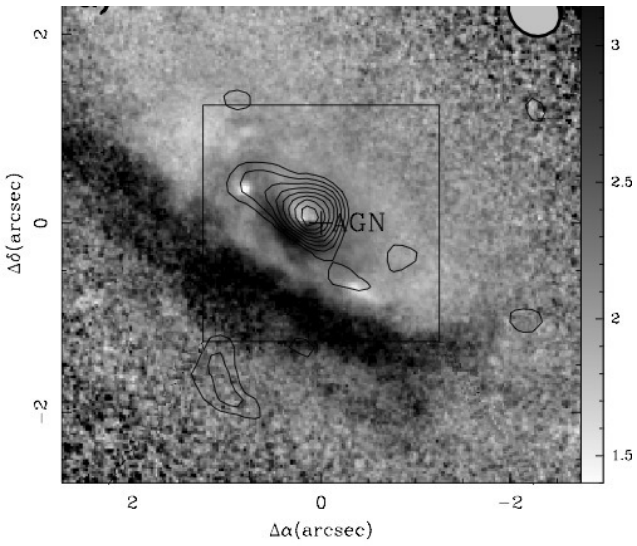

Fig. 1 $V-H$ color map of 3C 236, with the ^{12}CO(2-1) emission overlaid.

2 Continuum and CO emission

2.1 3C 236

The 1 mm and 3 mm continuum emission of 3C 236 consist of a bright central component plus a fainter component, located 0.8″ to the NW. The VLBI 1.7 and 5 GHz maps show that the location of these components correspond to the radio core and NW radio jet coordinates respectively (Taylor et al. 2001). Both the mm emission of the radio core and jet components of 3C 236 are consistent with synchrotron radiation (e.g., O'Dea 1998). The CO emission of 3C 236 comes from a 2.6 kpc diameter molecular gas disk. It rotates at $v \simeq 400$ km s^{-1} on the edges, and has $M(H_2) = 2.1\times10^9$ $M_\odot$. The molecular gas disk is associated with a highly inclined dust disk identified in the $V-H$ color map (Fig. 1) of the host galaxy (Allen et al. 2002; Floyd et al. 2008). The kinematics of the molecular gas disk are consistent with circular rotation, with no evidence of outflow signatures. However, based on the limits imposed by the sensitivity and velocity coverage of our data, we cannot exclude, in 3C 236, the existence of a molecular gas outflow comparable to the one detected in Mrk 231 (e.g. Feruglio et al. 2010).

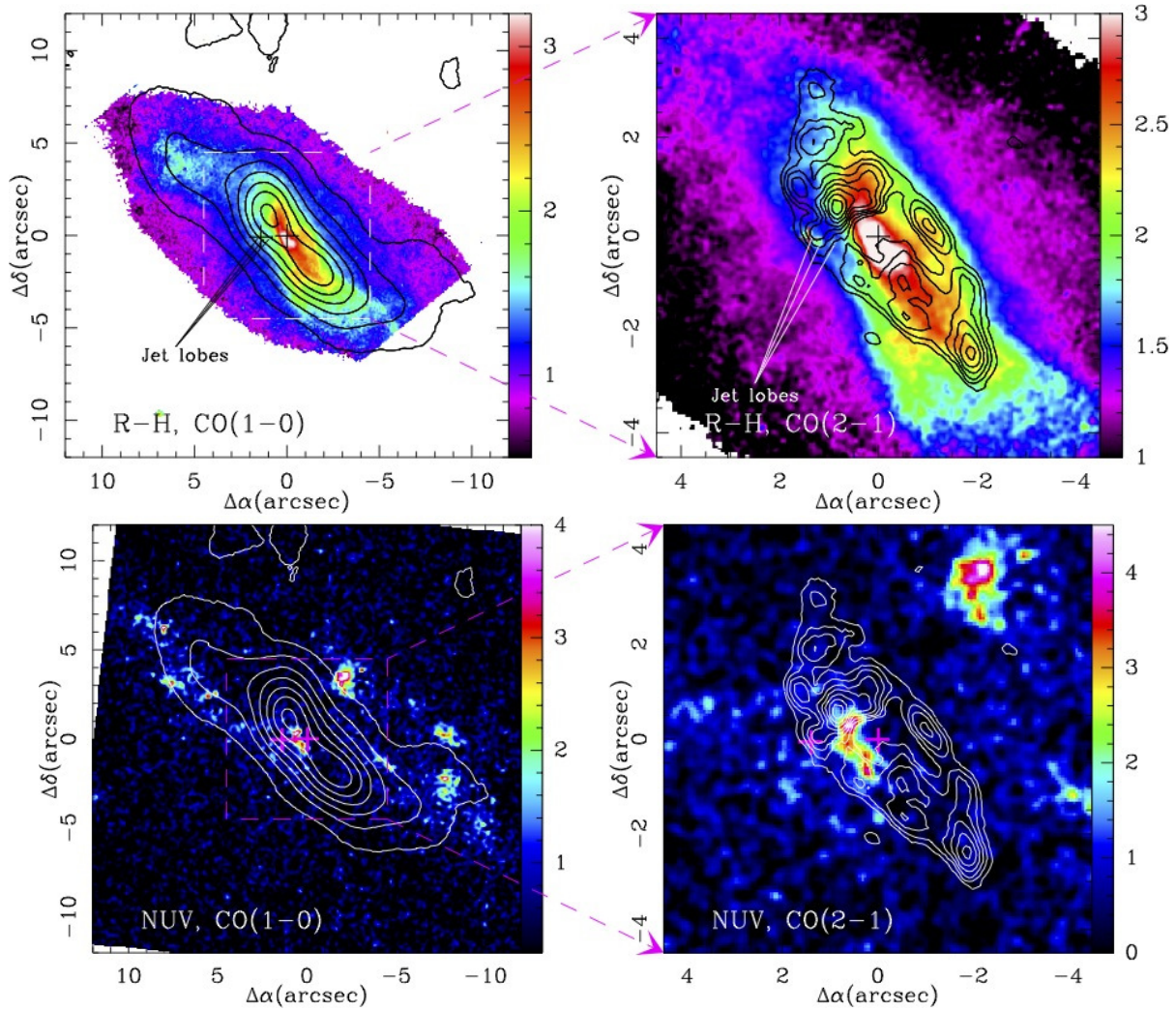

Fig. 2 *Left panels*: $R - H$ image of 3C 293, with the ^{12}CO(1-0) and ^{12}CO(2-1) emission overlaid. Crosses (+) mark the position of the AGN and jet peak emission. Solid lines mark the location of the IR counterparts of the Eastern radio lobe. *Right panels*: NUV image of 3C 293, with the ^{12}CO(1-0) and ^{12}CO(2-1) emission overlaid.

2.2 3C 293

The continuum emission of 3C 293, at 1 mm and 3 mm, consists of a bright central component (responsible for 86 % and 72 % of the total 1 and 3 mm emission, respectively) plus a fainter component ∼1.3″ to the east (PA = 89°). The coordinates of both components are consistent with the location of the radio core and eastern jet in the 1.35 and 1.5 GHz VLBI and MERLIN maps (Beswick et al. 2004). The 1 mm and 3 mm continuum emission from the radio core and the jet are both consistent with synchrotron emission, and with the results of Floyd et al. (2006), who showed that the emission from the jet was caused by synchrotron radiation even at NIR wavelengths. The CO emission of 3C 293 comes from a 21 kpc diameter, warped, corrugated disk, with the outer edges ($R \geq 8$ kpc) seen almost edge-on, and the central ($R \leq 4$ kpc) region tilted toward the plane of the sky, with the southern side facing us. The total molecular gas mass of the disk is $M(H_2) = 2.2{\times}10^{10}$ $M_\odot$. The disk is clearly associated with the dust and star formation regions of the host (Fig. 2). The kinematics of the CO lines show no evidence of fast (≥ 500 km s^{-1}) outflowing molecular gas in 3C 293.

3 Star formation rates and efficiencies

SFR estimations in active galaxies can be affected by the presence of AGN radiation and jet-induced shocks in the ISM, as these may increase the flux of ionized gas emission lines, vary the shape of the continuum, and destroy ISM molecules like the PAH. We have studied all SFR tracers available for 3C 236 and 3C 293, to constrain the potential biases inherent to the different SFR calibrations, and to search for the most accurate values of their SFR. Table 1 and Fig. 3 summarize our results.

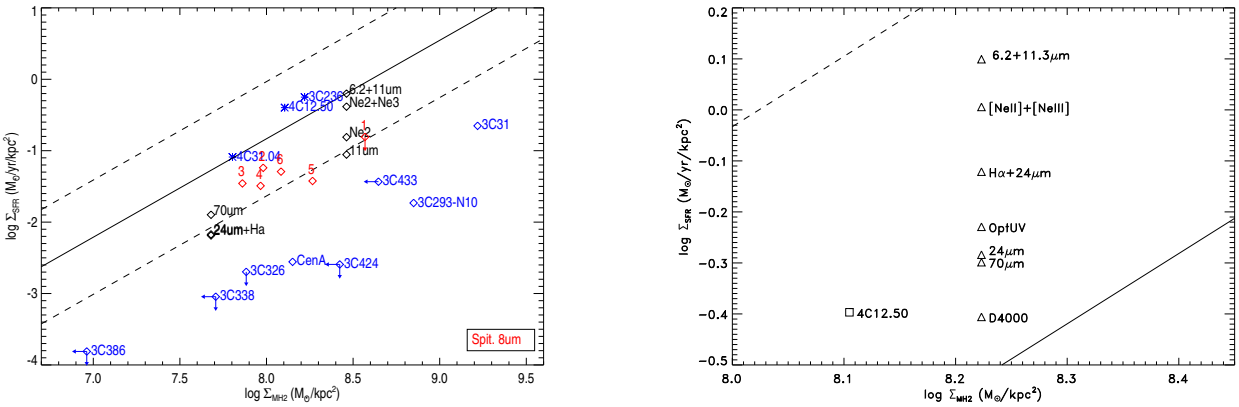

Fig. 3 *Left panel:* $\Sigma_{\rm SFR}$ and $\Sigma_{\rm MH_2}$ of 3C 293 (black and red), the sample of Nesvadba et al. (2010) (blue diamonds), young sources 4C 12.50, 4C 31.04, and 3C 236 (blue stars). Red diamonds show the SFR estimations based on Spitzer $S^{\rm dust}_{8\,\mu{\rm m}}$ data for 3C 293. Black diamonds show the SFR estimates for 3C 293 using the rest of tracers discussed in the text. Solid line: best-fit of the KS-law from Kennicutt (1998b). Dashed lines: dispersion around the KS-law best fit for normal star-forming galaxies (Roussel et al. 2007). $\Sigma_{\rm SFR}$ = SFR/area, $\Sigma_{\rm MH_2}$ = $M(H_2)$/area, *Right panel:* Zoom to the region around the 3C 236 SFE estimations (triangles).

3.1 3C 236

UV and optical photometry shows the presence of several knots of young star formation in 3C 236, with a SFR of 7.51 $M_\odot\,yr^{-1}$ (Tremblay et al. 2010). These regions are distributed along the nearest edge of the molecular gas disk and in the center of the galaxy, while the rest of the galaxy shows no UV emission. This morphology, strongly asymmetrical with respect to the galaxy major axis, suggests that there is a strong extinction in the molecular gas (and dust) disk. Thus, the SFR estimate of Tremblay et al. (2010) is probably a lower limit of the total SFR of 3C 236. Tremblay et al. (2010) showed that the contribution from emission lines to their UV and optical bands is negligible for 3C 236. The optical spectrum of the source shows no evidence of a significant AGN contribution (Holt et al. 2007). The geometry of 3C 236 also indicates that the star forming regions are unrelated to the jets. Thus, the UV and optical emission from the star-forming regions of 3C 236 has a negligible contribution from the AGN. The value derived for the SFR from these tracers is in all likelihood not significantly biased.

Based on the Hα emission (Kennicutt 1998b) and the 4000 Å break (D4000, Balogh et al. 1999), optical spectroscopy yields a SFR between 1 and 10 $M_\odot\,yr^{-1}$, consistent with the results from photometry. Both Hα and D4000 show an AGN contribution below 10 % in 3C 236. Using the SFR calibrations from Calzetti et al. (2007), Kennicutt et al. (2009), and Dicken et al. (2010), the 24 μm and 70 μm continuum emission of 3C 236 (which are dominated by star formation, Dicken et al. 2010), yield SFR = 6.62 $M_\odot\,yr^{-1}$ and SFR = 9.6±1.7 $M_\odot\,yr^{-1}$ respectively. The SFR derived from the 24 μm and 70 μm are consistent with each other and with the SFR estimations above, supporting that the contribution from the AGN to these fluxes is small, and the SFR estimations from the IR continuum are accurate. The [Ne III] λ15.6 μm and [Ne II] λ12.8 μm emission of 3C 236 yield SFR = 16±1 $M_\odot\,yr^{-1}$. The infrared emission-line ratios of 3C 236 (Genzel et al. 1998; Pereira-Santaella et al. 2010; Willett et al. 2010) show that the AGN contribution to the Neon lines is below 20 %, consistent with the samples of star-formation dominated galaxies.

The 6.2 μm plus 11.3 μm PAH emission of 3C 236 yields 11 $M_\odot\,yr^{-1} \leq$ SFR $\leq$ 22 $M_\odot\,yr^{-1}$, consistent with the estimations reported above. The 7.7 μm PAH emission yields SFR $\leq$ 0.23 $M_\odot\,yr^{-1}$, much lower than any other SFR estimation, and consistent with the SFR estimated for the rhe radio galaxies presented in Nesvadba et al. (2010) radio galaxies (which were also calculated using the 7.7 μm emission) with H_2 masses $\sim 10^9$ $M_\odot$. However, it is known that active galaxies show low 7.7 μm emission compared with normal (KS) star forming galaxies, probably due to the destruction of smaller PAH by shocks and/or radiation from the AGN (O'Dowd et al. 2009). Leaving aside the estimate derived from the 7.7 μm PAH feature, as it is likely an underestimation, we conclude that the average value of the SFR of 3C 236, obtained from all the different tracers discussed above, is SFR $\sim$ 9.2 $M_\odot\,yr^{-1}$. Based on this SFR, and its $M(H_2)$, 3C 236 has a SFE consistent with the SFE of normal star-forming galaxies, and 10 to 50 times higher than the SFE of radio galaxies from Nesvadba et al. (2010).

3C 236 is a re-activated AGN with a young CSS radio component, while the rest of sources in the Nesvadba et al. (2010) sample are old, evolved galaxies. A literature search shows that there are two other young sources with SFR and $M(H_2)$ data available: 4C 12.50 (Dasyra & Combes 2012) and 4C 1.04 (García-Burillo et al. 2007). The SFE of these two sources is also consistent with the SFE of normal star forming galaxies, suggesting that the quenching of the star formation could be related to the age of the radio source. Tadhunter (these proceedings) suggests that star formation could be more common in GPS/CSS sources than in large sources. On the other hand, O'Dea (these proceedings) shows that the higher star formation found in GPS/CSS sources may be just a selection effect.

Table 1 SFR and $M(H_2)$ estimations.

3C 236	SFR ($M_\odot\,yr^{-1}$)	$M(H_2)$ ($10^8\,M_\odot$)	Area (kpc^2)
Optical+UV	7.51	21.3	12.7
Hα	1.0	21.3	12.7
D4000	1–10	21.3	12.7
24 μm	6.62	21.3	12.7
24 μm+Hα	9.6±1.7	21.3	12.7
70 μm	3–10	21.3	12.7
7.7 μm	<0.24	21.3	12.7
6.2+11.3 μm	11-22	21.3	12.7
Ne II + Ne III	12.9±0.5	21.3	12.7
3C 293		($10^9\,M_\odot$)	
24 μm	3.0	22	460
24 μm+Hα	3.2±0.1	3.3	5.4[a]
70 μm	5.9±0.1	22	460
11.3 μm	2.5±0.2	8.2	28.3
6.2+11.3 μm	18±1	8.2	28.3
Ne II	4.4±1	8.2	28.3
Ne II + Ne III	11±1	8.2	28.3
$S_{8\,\mu m}^{dust}$	<3.3	8.0	21.5
$S_{8\,\mu m}^{dust}$	1.4	1.9	19.7
$S_{8\,\mu m}^{dust}$	1.0	2.2	30.0
$S_{8\,\mu m}^{dust}$	1.7	4.8	51.8
$S_{8\,\mu m}^{dust}$	0.5	2.5	13.5
$S_{8\,\mu m}^{dust}$	0.5	1.1	9.3

Notes. Limits are 3σ; uncertainties in $M(H_2)$ are $\sim 5\,\%$; SFR uncertainties listed when available. The last rows of 3C 293 (8 μm, dust) correspond to SFR measurements in different regions of the galaxy.

[a] The area of the 24 μm measurement corresponds to the unresolved galaxy (460 kpc^2).

3.2 3C 293

3C 293 is an old radio source, which was included in the Nesvadba et al. (2010) sample. Even though it has large contents of molecular gas and young stars, Nesvadba et al. (2010) measured an SFE 20 times lower than expected for normal star-forming galaxies based on its 7.7 μm PAH emission and the H_2 measurements of Evans et al. (1999). On the other hand, the FIR luminosity of 3C 293 is consistent with FIR luminosities of normal, KS-law, star-forming galaxies with similar molecular gas contents, suggesting that the SFR of 3C 293 calculated with the 7.7 μm PAH emission could be underestimated. 3C 293 is thus a great source to test if the age of the radio activity is related to the SFE of hosts of radio galaxies, as well as to re-examine the SFE estimations with our higher resolution and sensitivity data.

The UV emission of 3C 293 shows a clumpy distribution of star formation regions associated with the molecular gas disk (Fig. 2). The heavy obscuration seen in the $R-H$ map, and the patchy morphology of the NUV emission suggest that any SFR estimations based on the NUV image will be largely underestimated. The optical data available for 3C 293 are also affected by heavy obscuration, plus large contributions from the AGN. Hence, it was not possible to obtain accurate SFR estimations based on the UV or optical data of 3C 293. The continuum and line mid-infrared emission of 3C 293 is dominated by star formation, and the shape of the continuum is similar to the continuum of local star-forming galaxies (Smith et al. 2007).

Using a similar analysis as for 3C 236, the IR continuum emission of 3C 293 yields SFR = 3.0 $M_\odot\,yr^{-1}$ and SFR = 3.2±0.1 $M_\odot\,yr^{-1}$ for the 24 μm and 24 μm+Hα, respectively. The ionized gas emission lines yield SFR = 4.4±1 $M_\odot\,yr^{-1}$ and SFR = 11±1 $M_\odot\,yr^{-1}$ for the [Ne II] and [Ne II]+[Ne III] relations, respectively. The PAH emission of 3C 293 yield SFR = 18±1 $M_\odot\,yr^{-1}$ for the 6.3+11.3 μm PAH combined, and SFR = 2.5±0.2 $M_\odot\,yr^{-1}$ using only the 11.3 μm PAH emission. Therefore, our SFR and $M(H_2)$ estimations for 3C 293 are consistent with KS-law efficiencies, the SFE of young sources, and 20 times larger than the SFE estimated by Nesvadba et al. (2010).

Nesvadba et al. (2010) estimated the SFR of 3C 293 using the 7.7 μm PAH emission as a proxy of $S_{8\,\mu m}^{dust}$ in the Calzetti et al. (2007) SFR calibration, where $S_{8\,\mu m}^{dust}$ is the luminosity surface density in the IRAC 8 μm image, with the stellar continuum removed using the IRAC 3.6 μm image (Calzetti et al. 2005; Helou et al. 2004). If the SFR of 3C 293 is calculated using the $S_{8\,\mu m}^{dust}$ relation described above, instead of the 7.7 μm PAH emission, it increases by a factor of ~ 6. This new value of the SFR yields a SFE lower than the SFE of normal (KS-law) star forming galaxies, however. The molecular gas density used by Nesvadba et al. (2010) comes from CO observations by Evans et al. (1999), who argued that the molecular gas of 3C 293 was distributed over a 6 kpc-diameter disk. Our higher resolution maps show that the area of the disk is 9 times larger. Combining the SFR estimation using $S_{8\,\mu m}^{dust}$, with the larger H_2 disk, we obtained a SFE in 3C 293 consistent with the KS-law.

Contrary to 3C 236, 4C 12.50, and 4C 31.04, the jets of 3C 293 have had enough time to affect the star formation in the host. Thus, a diminished SFE would be expected. The SFE of 3C 293 is consistent with that of normal star-forming galaxies and young radio sources, with no evidence of quenched star formation, however. Our results suggest that the apparently low SFE found in evolved radio galaxies is probably caused by an underestimation of the SFR and/or an overestimation of the H_2 density, instead of being a distinctive property of these sources. New observations of cold molecular gas in the ISM of young and evolved radio galaxies, and accurate measurements of their SFR, are key to understanding how AGN feedback affects the properties of their hosts.

References

Akujor, C. E., Leahy, J. P., Garrington, S. T., et al. 1996, MNRAS, 278, 1

Allen, M. G., Groves, B. A., Dopita, M. A., Sutherland, R. S., Kewley, L. J. 2008, ApJS, 178, 20

Allen, M. G., Sparks, W. B., Koekemoer, A., et al. 2002, ApJS, 139, 411

Balogh, M. L., Morris, S. L., Yee, H. K. C., Carlberg, R. G., & Ellingson, E. 1999, ApJ, 527, 54

Baldi, R. D. & Capetti, A. 2008, A&A, 489, 989

Barthel, P. D., Miley, G. K., Jagers, W. J., Schilizzi, R. T., & Strom, R. G. 1985, A&A, 148, 243

Beswick, R. J., Peck, A. B., Taylor, G. B., & Giovannini, G. 2004, MNRAS, 352, 49

Calzetti, D., Kennicutt, R. C., Engelbracht, C. W., et al. 2007, ApJ, 666, 870

Calzetti, D., Kennicutt, R. C., Bianchi, L., et al. 2005, ApJ, 633, 871

Capetti, A., de Ruiter, H. R., Fanti, R., et al. 2000, A&A, 362, 871

Dasyra, K. M. & Combes, F. 2011, A&A, 533, L10

Dasyra, K. M. & Combes, F. 2012, A&A, 541, L7

de Koff, S., Best, P., Baum, S. A., et al. 2000, ApJS, 129, 33

Dicken, D., Tadhunter, C., Axon, D., et al. 2010, ApJ, 722, 1333

Emonts, B. H. C., Morganti, R., Tadhunter, C. N., et al. 2005, MNRAS, 362, 931

Evans, A. S., Sanders, D. B., Surace, J. A., & Mazzarella, J. M. 1999, ApJ, 511, 730

Fanaroff, B. L. & Riley, J. M. 1974, MNRAS, 167, 31P

Floyd, D. J. E., Perlman, E., Leahy, J. P., et al. 2006, ApJ, 639, 23

Floyd, D. J. E., Axon, D., Baum, S., et al. 2008, ApJS, 177, 148

García-Burillo, S., Combes, F., Neri, R., et al. 2007, A&A, 468, L71

Genzel, R., Lutz, D., Sturm, E., et al. 1998, ApJ, 498, 579

Guilloteau, S., Delannoy, J., Downes, D., et al. 1992, A&A, 262, 624

Helou, G., Roussel, H., Appleton, P., et al. 2004, ApJS, 154, 253

Holt, J., Tadhunter, C. N., & Morganti, R. 2006, AN, 327, 147

Holt, J., Tadhunter, C. N., Gonzlez Delgado, R. M., et al. 2007, MNRAS, 381, 611

Joshi, S. A., Saikia, D. J., Ishwara-Chandra, C. H., & Konar, C. 2011, MNRAS, 414, 1397

Kennicutt, Jr., R. C. 1998a, ARA&A, 36, 189

Kennicutt, Jr., R. C. 1998b, ApJ, 498, 541

Kennicutt, Jr., R. C., et al. 2009, ApJ, 703, 1672

Labiano, A., García-Burillo, S., Combes, F., et al. 2013, A&A, 549, 58

Labiano, A., García-Burillo, S., Combes, F., et al. 2014, A&A, 564, 128

Lehnert, M.D., Tasse, C., Nesvadba, N.P.H., Best, P.N., & van Driel, W. 2011, A&A, 532, L3

Leipski, C., Antonucci, R., Ogle, P., & Whysong, D. 2009, ApJ, 701, 891

Machalski, J.; Koziel-Wierzbowska, D., Jamrozy, M., & Saikia, D.J. 2008, ApJ, 679, 149

Mahony, E.K., Morganti, R., Emonts, B.H.C., Oosterloo, T.A., & Tadhunter, C. 2013, MNRAS, 435, L58

Martel, A.R., Baum, S.A., Sparks, W.B., et al. 1999, ApJS, 122, 81

Massaro, F., Harris, D.E., Tremblay, G.R., et al. ApJ, 714, 589

Morganti, R., Oosterloo, T.A., Emonts, B.H.C., van der Hulst, J.M., & Tadhunter, C.N. 2003, ApJ, 593, L69

Morganti, R., Tadhunter, C.N., & Oosterloo, T.A. 2005, A&A, 444, L9

Nesvadba, N.P.H., Boulanger, F., Salomé, P., et al. 2010, A&A, 521, 65

Nesvadba, N.P.H., Lehnert, M.D., De Breuck, C., Gilbert, A.M., & van Breugel, W. 2008, A&A, 491, 407

Nesvadba, N.P.H., Lehnert, M.D., Eisenhauer, F., et al. 2006, A&A, 650, 693

O'Dea, C.P., Koekemoer, A.M., Baum, S.A., et al. 2001, AJ, 121, 1915

O'Dea, C.P. 1998, PASP, 110, 493

O'Dowd, M.J., Schiminovich, D., Johnson, B.D., et al. 2009, ApJ, 705, 885

Papadopoulos, P.P., van der Werf, P., Isaak, K., & Xilouris, E.M. 2010, ApJ, 715, 775

Pereira-Santaella, M., Diamond-Stanic, A.M., Alonso-Herrero, A., & Rieke, G.H. 2010, ApJ, 725, 2270

Roussel, H., Helou, G., Hollenbach, D.J., et al. 2007, ApJ, 669, 959

Rupke, D.S., Veilleux, S., & Sanders, D.B. 2005, ApJ, 632, 751

Schilizzi, R.T., Tian, W.W., Conway, J.E., et al. 2001, A&A, 368, 398

Schmidt, M. 1959, ApJ, 129, 243

Smith, J.D.T., Draine, B.T., Dale, D.A., et al. 2007, ApJ, 656, 770

Tadhunter, C., Holt, J., González Delgado, R., et al. 2011, MNRAS, 412, 960

Tadhunter, C., Robinson, T.G., Gonzáles Delgado, R.M., Wills, K., & Morganti, R. 2005, MNRAS, 356, 480

Taylor, G.B., Hough, D.H., & Venturi, T. 2001, ApJ, 559, 703

Tremblay, G.R., O'Dea, C.P., Baum, S.A., et al. 2010, ApJ, 715, 172

Willett, K.W., Stocke, J.T., Darling, J., & Perlman, E.S. 2010, ApJ, 713, 1393

Willis, A.G., Strom, R.G., & Wilson, A.S. 1974, Nature, 250, 625